Hindawi
Journal of Chemistry
Volume 2021, Article ID 4413095, 9 pages
https://doi.org/10.1155/2021/4413095

Research Article

Adsorption of Chromium (VI) by Cu (I)-MOF in Water: Optimization, Kinetics, and Thermodynamics

Hongxue Qi, Xianjun Niu, Haipeng Wu, Xiuping Liu, and Yongqiang Chen

School of Chemistry and Chemical Engineering, Jinzhong University, Jinzhong 030619, Shanxi, China

Correspondence should be addressed to Yongqiang Chen; chenyongqiang82@126.com

Received 30 August 2021; Accepted 3 December 2021; Published 24 December 2021

Academic Editor: Gang Feng

To investigate the adsorption behavior of Cu (I)-MOF material for chromium (VI) in water, the parameters of influencing adsorption were optimized and found as follows: the optimal pH was 6 for the adsorption of Cr (VI) by the Cu (I)-MOF, the optimal amount of adsorbent was 0.45 $g{\cdot}L^{-1}$, and the adsorption saturation time was within 180 min. Subsequently, the kinetics results were fitted by four models such as pseudo-first-order, pseudo-second-order, Elovich, and intraparticle diffusion models. Among them, the adsorption of chromium (VI) was more inclined to the pseudo-first-order model ($R_{adj}{}^2 = 0.9230$). Then, the isotherm data were fitted by Langmuir and Freundlich models. The results indicated that Langmuir isotherm was the excellent match model ($R_{adj}{}^2 = 0.9827$). It belongs to a monolayer adsorption, and the maximum adsorption capacity was 95.92 $mg{\cdot}g^{-1}$. Subsequently, the thermodynamic parameters of the adsorption were calculated as follows: enthalpy change (ΔH^{θ}) was −8.583 $kJ{\cdot}mol^{-1}$, entropy change (ΔS^{θ}) was −8.243 $J{\cdot}mol^{-1}\,K^{-1}$, and the Gibbs function change (ΔG^{θ}) was less than zero in the temperature range of 288–328 K, indicating that the reaction was spontaneous. Finally, both the spectra of infrared and XPS supported the adsorption mechanism that belonged the ion exchange. The spectra of XRD and SEM images shown that the structure of Cu (I)-MOF remained stable for at least 3 cycles. In conclusion, Cu (I)-MOF material has a high adsorption capacity, good water stability, low cost, and easy to prepare in large quantities in practical application. It will be a promising adsorbent for the removal of Cr (VI) from water.

1. Introduction

Heavy metal chromium pollution has become a serious environmental problem worldwide. Mineral mining, electroplating, leather tanning, and other industrial processes have resulted in a large amount of wastewater containing chromium [1]. It has been listed as a carcinogen by the International Agency for Research on Cancer of the World Health Organization [2]. The hexavalent chromium (Cr (VI)) and trivalent chromium (Cr (III)) ions were the main stable forms in the water, the toxicity of Cr (VI) was about 100 times higher than that of Cr (III), and high content of Cr (VI) will be highly toxic, carcinogenic, and mutagenic properties [3]. Excessive levels of Cr (VI) in drinking water will harm human health and cause the digestive system and liver damage [4]. In addition, wastewater containing chromium compounds can reduce the efficiency of the biochemical treatment system. Therefore, Cr (VI) is the optimal control of pollutants in wastewater [5] and must be treated before discharge into the environment to reduce the harm to environment [6].

Treatment methods for Cr (VI) ions in water include chemical reduction, electrolysis, ion exchange, phytoremediation, and adsorption [7]. Among them, the adsorption method is widely used for the elimination of heavy metals from polluted water because of its simple operation, low cost, and less required equipment. The choice of material is very crucial for adsorption; in addition to the activated carbon, silica gel, and other traditional materials, the modified materials or new materials should be developed to improve the adsorption performance, such as chitosan [8] and its magnetic materials [9], graphene and its composites [10], nano zero-valent iron [11], and metal-organic framework (MOF) materials [12].

Compared with other materials, MOF is a new class of porous structures composed of different varieties transition metal ions (or clusters). To date, MOFs have exhibited numerous properties, such as gas adsorption, separations, sensors, drug delivery, and catalytic activity [13–15]. Numerous studies have been conducted on MOF for the removal of heavy metals from water bodies [16]. Particularly, the MOF can be used for the high efficiency removal of Cr (VI) in aqueous solution [17–19]. But some MOFs are not stable in water or difficult to produce in large quantities in practical application. A Cu (I)-MOF, $(Cu[2,4,6\text{-tris}(4\text{-pyridyl})pyridine]\cdot NO_3\cdot CH_3OH)_\infty$, previously synthesized with a 4-fold helical channels (Figure 1) and different inorganic anions can be recognized in water via color change [20]. Cu (I)-MOF is very suitable for application in water treatment because it has very good water stability and is easy to produce in large quantities in practical application. However, the identification of heavy metals has not been studied. In this study, the adsorption behavior for Cr (VI) was investigated in aqueous solution related to the optimization, kinetics, thermodynamics, and mechanism studies.

2. Materials and Methods

2.1. Materials. Ammonia, methanol, and potassium dichromate ($K_2Cr_2O_7$, 99.9%) were obtained from Tianjin Beichen Founder Reagent Factory, copper nitrate trihydrate and *N*,*N*-dimethylacetamide (analytical pure) were purchased from Tianjin Komil Chemical Reagent Co., Ltd., magnetic stirrer (DF-101S) was from Zhengzhou Biochemical Instrument Factory, microscope (OST-BH200) was from Suzhou OST optical instrument Co., Ltd., and flame atomic absorption spectrophotometry was made in Beijing PERSEE General Instrument Co., Ltd.

2.2. Preparation of Cu (I)-MOF. The Cu (I)-MOF was synthesized using a hydrothermal method as reported by the previous work [20]. Briefly, 0.031 g of ligand (2,4,6-tris (4-pyridyl) pyridine) and 0.072 g of copper nitrate trihydrate were added into 100 mL reaction kettles, and then 10 mL of mixed solvent (*N*, *N*-dimethylacetamide and methanol, volume ratio is 1 : 1) was added. The reaction kettle was shaken well, screwed down, and put in the oven at 120°C for 72 h. Allow cooling to room temperature, cleaned with methanol, and orange crystals obtained. Then, it was dried at room temperature and stored to use.

2.3. Adsorption Experiments. The experiments were conducted to assess the effects of various parameters on Cr (VI) adsorption onto Cu (I)-MOF. Briefly, (1) pH was adjusted to 4, 5, 6, 7, and 8 using a certain amount of dilute HCl or NaOH solution; (2) adsorbent dosage: 0.15, 0.30, 0.45, 0.60, and 0.75g·L^{-1}; (3) contact time: 5, 10, 20, 30, 60, 120, and 720 min; (4) initial Cr (VI) concentration: 25, 50, 100, 200, and 250 mg·L^{-1}; and (5) temperature: 288, 298, 308, 318, and 328 K. Each adsorption experiment was carried out by mixing a weighted amount of Cu (I)-MOF with 100 mL of Cr (VI) solution in a 100 mL beaker. The mixture was shaken by magnetic stirring (120 rpm) at a definite temperature for a proper time. The supernatant fluid was obtained through the centrifuge, and the concentrations of Cr (VI) were analyzed using the flame atomic absorption spectrometer. The adsorption capacity was calculated according to the following equation:

$$q_e = \frac{(c_0 - c_t)V}{m}, \tag{1}$$

where q_e is the adsorption capacity at equilibrium (mg·g^{-1}), c_0 is the initial concentration of Cr (VI) ionic solution, c_t is the concentration after adsorption time t (mg·L^{-1}), m is the mass of adsorbent (g), and V is the volume of Cr (VI) solution (L).

2.4. Kinetics Models

2.4.1. Pseudo-First-Order Equation.

$$q_t = q_e\left(1 - e^{-k_1 t}\right), \tag{2}$$

where q_e is the same as in equation (1), q_t is the adsorption capacity of the adsorbent on chromium (VI) ion at any time t (mg·g^{-1}), and k_1 is the rate constant of the pseudo-first-order equation (min^{-1}) [21].

2.4.2. Pseudo-Second-Order Equation.

$$q_t = \frac{k_2 q_e^2 t}{1 + k_2 q_e t}, \tag{3}$$

where t, q_t, and q_e are the same as in equation (2), and k_2 is the rate constant of the pseudo-second-order equation (g·mg^{-1}·min) [22].

2.5. Elovich Model.

$$q_t = \frac{1}{\beta}\ln(1 + \alpha\beta t), \tag{4}$$

where t and q_t are the same as in equation (2), α is the initial rate constant (mg·g^{-1}·min), and β is the desorption coefficient (mg·g^{-1}) [23].

2.6. Intraparticle Diffusion Model.

$$q_t = k_p t^{0.5} + C, \tag{5}$$

where t and q_t are the same as in equation (2), k_p is the rate constant of the intraparticle diffusion model (mg·g^{-1}·min), and C is a constant related to the thickness of the boundary layer (mg·g^{-1}) [24].

2.7. Isotherm Models

2.7.1. Langmuir Model.

$$q_e = \frac{q_m \cdot K_L \cdot c_e}{1 + K_L \cdot c_e}, \tag{6}$$

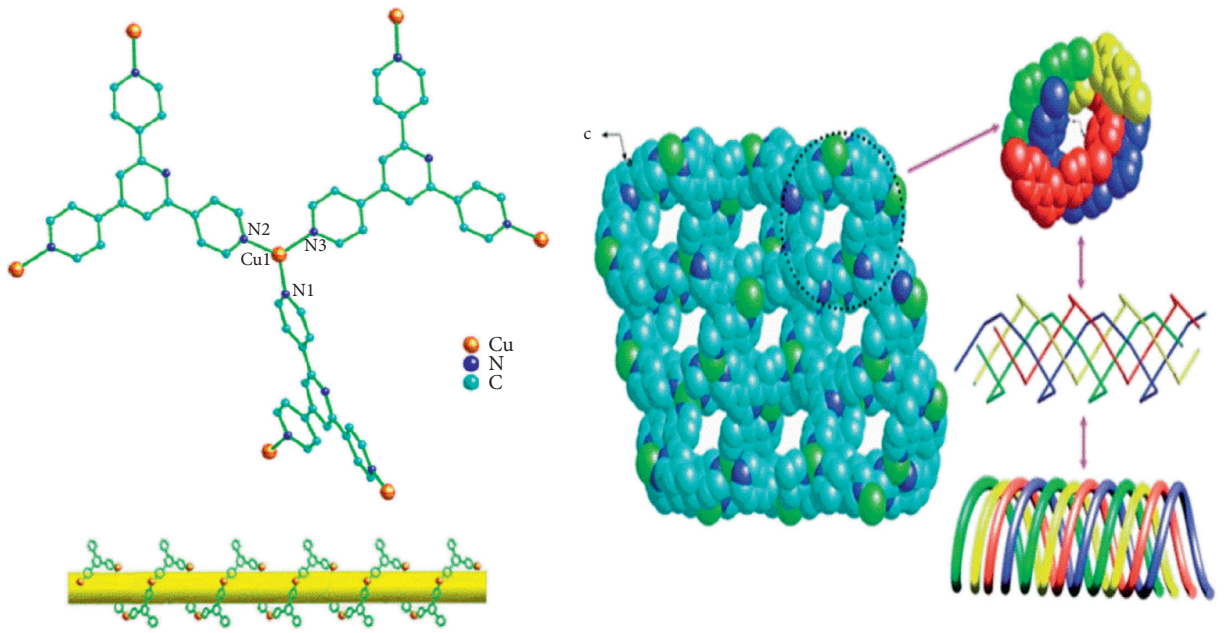

Figure 1: Diagram of Cu (I)-MOF and its 4-fold helical channel [20].

where q_e is the same as in equation (1), c_e is the concentration of adsorbate in equilibrium solution (mg·L^{-1}), q_m is the maximum adsorption capacity of the adsorbent (mg·g^{-1}), and K_L is the Langmuir adsorption constant (L·mg^{-1}), which is related to the affinity of binding sites [25].

2.7.2. Freundlich Model.

$$q_e = K_F \cdot c_e^{1/n}, \tag{7}$$

where q_e and c_e are the same as in equation (6), K_F is Freundlich adsorption constant ((mg·g^{-1}) (L·mg^{-1}) n), and the adsorption index $1/n$ can reflect the extent of the adsorption reaction. If the value of $1/n$ is between 0.1 and 0.5, the adsorption is favorable; if $1/n$ is greater than 1, it is unfavorable; if $1/n$ is zero, it is irreversible [26].

2.8. Adsorption Thermodynamics.

$$\ln K_e^\theta = \frac{\Delta S^\theta}{R} - \frac{\Delta H^\theta}{R} \cdot \frac{1}{T}, \tag{8}$$

$$K_e^\theta = \frac{K_L \cdot C_{\text{adsorbate}}^\theta}{\gamma_{\text{adsorbate}}}, \tag{9}$$

$$\Delta G^\theta = \Delta H^\theta - T \cdot \Delta S^\theta, \tag{10}$$

where K_e^θ is the thermodynamic equilibrium constant (dimensionless) [27], ΔS^θ is the reaction entropy change (J·mol^{-1}·K^{-1}), ΔH^θ is the reaction enthalpy change (kJ·mol^{-1}), R and T are the same as in equation (5), K_L is the Langmuir equilibrium constant (L·mg^{-1}), $C_{\text{Adsorbate}}^\theta$ is the unitary standard concentration of the adsorbate (1 mol·L^{-1}), $\gamma_{\text{adsorbate}}$ is the coefficient of activity (dimensionless), and ΔG^θ is the Gibbs function change (kJ·mol^{-1}). The values of reaction enthalpy change (ΔH^θ) and entropy change (ΔS^θ) were calculated from the slope and intercept obtained by $1/T$ versus $\ln K_e^\theta$ plot.

2.9. Characterization. The infrared spectra of surface functional groups of samples were investigated using Fourier transform infrared spectroscopy (WQF-510A, Beijing Rayleigh Analytical Instrument Co., Ltd.) with wave numbers from 4000 to 500 cm^{-1}. The spectra of XPS were measured with the Thermos Scientific K-Alpha XPS spectrometer. The powder XRD spectra of the samples were performed by X-ray diffraction (XRD-6100, Shimadzu) using Cu Kα radiation ($\lambda = 1.5406$ Å), employing a scan step of 0.02° in the 2θ ranged from 5° to 40°. The morphology of samples was observed by using a scanning electron microscope (SEM, JSM-7001F).

3. Results and Discussion

3.1. Optimization of Adsorption Conditions

3.1.1. Effect of pH. The pH value of the solution will affect the types, binding sites, valence state, and surface charge of metal ions, even the arrangement of molecular structure [28]. Cr (VI) adsorption capacity at various pH values was performed after equilibration with Cu (I)-MOF. As shown in Figure 2, the adsorption capacities decreased with the increase of the pH value. A similar tendency was reported on Cr (VI) adsorption [29]. Although the maximum adsorption amount has been achieved at pH 4.0 experimentally, the pH of 6.0 was selected for next experiments. Because, the pH value is required between 6 and 9 in the actual water treatment process according to the standard of wastewater discharge.

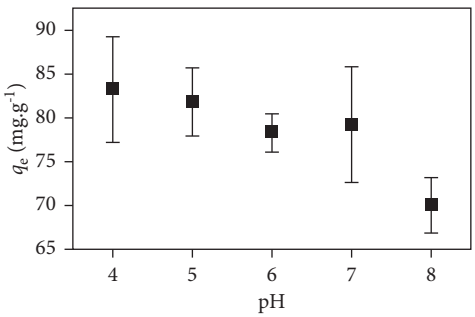

Figure 2: The effect of pH in water for chromium (VI) adsorption onto Cu (I)-MOF.

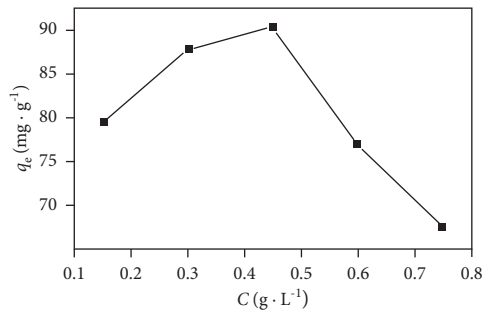

Figure 3: The effect of the amounts of Cu (I)-MOF for Cr (VI) adsorption in aqueous solution.

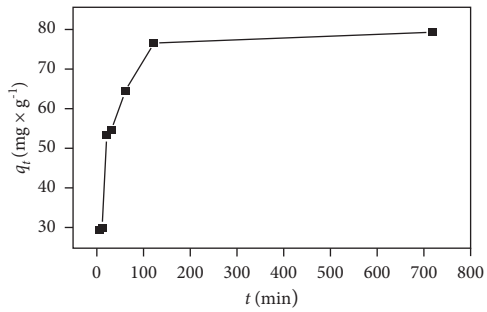

Figure 4: The curves of Cr (VI) adsorbed by Cu (I)-MOF at different times in aqueous solution.

3.1.2. Effect of Adsorbent Dosage. The amount of Cu (I)-MOF material directly affects the adsorption efficiency of Cr (VI) ions, and the dose selection will directly guide for the removal of Cr (VI) in the process of water treatment. As shown in Figure 3, at the early stage, the equilibrium adsorption amount was proportional to the amount of adsorbent. However, they were inversely proportional at the late stage. The former maybe explained by the sufficient surface area was available for the adsorption of Cr (VI), while the latter might be explained by the comparatively less available specific surface area with increase in adsorption of Cr (VI) ions. Therefore, 0.45 g·L^{-1} of Cu (I)-MOF material was selected as the optimal dosage for Cr (VI) ions adsorption for the next experiments.

3.1.3. Effect of Reaction Time. As shown in Figure 4, the rapid adsorption rate occurred within 120 minutes, and the adsorption capacity of Cr (VI) ions gradually reached equilibrium within 180 min. Because, Cu (I)-MOF material surface has the sufficient unsaturated sites at the initial stage of the adsorption. With the increase of time (>180 min), some adsorption sites bonded with Cr (VI), and the adsorption rate increased slowly and reached completely equilibrium at 720 min. Therefore, 180 min was selected as the optimal time for Cr (VI) ions adsorption in the next studies.

3.2. Adsorption Kinetics. The adsorption kinetics can provide the information on adsorption efficiency and reactor scale, which can provide the reference for the design parameters of water treatment equipment. To illustrate the adsorption kinetics, the adsorption experiments were performed at different times. The kinetic results fitted by four models included pseudo-first-order, pseudo-second-order, Elovich, and intraparticle diffusion model. The pseudo-first-order model can provide a simple monophasic description mathematically [21]. The pseudo-second-order model assumed that the adsorption rate is controlled by the chemisorption [22]. The Elovich model assumed that the active sites on solid surface are heterogeneous [23], and it can indicate the different activated energies for chemisorption. For the intraparticle diffusion model, it was usually used to estimate whether intraparticle diffusion, bulk diffusion, or film diffusion is the rate limiting step [24].

The parameters of the four models were calculated by nonlinear fitting approach to avoid expressive errors [30]. Based on the comparison of the values of the adjusted determination coefficients (R^2_{adj}), as given in Table 1, the pseudo-first-order model ($R^2 = 0.9230$) was the highest value among the four models, which indicated that the pseudo-first-order model was more suitable for the adsorption of Cr (VI) onto Cu (I)-MOF in aqueous solution.

3.3. Adsorption Isotherm. To elucidate the isotherm mechanism, the adsorption experiments were performed at different initial concentrations of Cr (VI). Cr (VI) adsorption by Cu (I)-MOF was investigated by two models included Langmuir and Freundlich. Briefly, the Langmuir adsorption isotherm model often describes as monolayer adsorption [25]; it assumes a uniform surface bond and no interaction with other adsorbate molecules. On the contrary, the Freundlich isotherm assumes that adsorbate molecules bond to the adsorbent on a multilayer surface and they are influenced by other adsorbates [26].

As given in Table 2, the highest degree of R^2_{adj} (0.9827) was related to the Langmuir model, which indicated that the adsorption of Cr (VI) was more inclined to the Langmuir model. Accordingly, adsorption behavior belonged to monolayer adsorption (homogeneous surface), and the Langmuir isotherm model predicted the maximum adsorption capacity of 95.92 mg·g^{-1}.

MOFs are hybrid materials composed of metal (oxide) cation clusters and multiple ligands. They have many advantages, such as large specific surface area, special metal

Table 1: Kinetic models of adsorption of Cr (VI) onto Cu (I)-MOF in aqueous solution.

Models	Parameters		R^2_{adj}
Pseudo-first-order	k_1 (min^{-1})	q_e ($mg{\cdot}g^{-1}$)	
	0.0547	53.95	0.9230
Pseudo-second-order	k_2 ($g{\cdot}mg^{-1}{\cdot}min$)	q_e ($mg{\cdot}g^{-1}$)	
	0.00129	58.72	0.8504
Elovich	α ($mg{\cdot}g^{-1}{\cdot}min$)	β ($mg{\cdot}g^{-1}$)	
	0.1218	24.38	0.5971
Intraparticle diffusion	k_p ($mg{\cdot}g^{-1}{\cdot}min$)	C ($mg{\cdot}g^{-1}$)	
	1.1812	28.97	0.2276

R^2_{adj} is the adjusted determination coefficient; k_1 is the first-order rate constant; q_e is the equilibrium adsorption capacity; k_2 is the second-order rate constant; α is the initial rate constant; β is the desorption coefficient; k_p is the rate constant; C is a constant related to the thickness of the boundary layer.

Table 2: Chromium (VI) adsorption isotherm fitting parameters for chromium (VI) by Cu (I)-MOF in aqueous solution.

Models	Parameters		R^2_{adj}
Langmuir	q_m ($mg{\cdot}g^{-1}$)	K_L ($L{\cdot}mg^{-1}$)	
	95.92	0.40995	0.9827
Freundlich	K_F (($mg{\cdot}g^{-1}$) ($L{\cdot}mg^{-1}$) n)	$1/n$	
	37.46	0.2185	0.8279

R^2_{adj} is the adjusted determination coefficient; q_m is the maximum adsorption capacity; K_L is the Langmuir adsorption constant; K_F is the Freundlich adsorption constant; $1/n$ is the adsorption constant.

sites, easy aperture adjustment, and easy surface modification. Compared with other materials (Table 3), Cu (I)-MOF material as adsorbent has a larger adsorption capacity, which was much higher than those of most adsorption materials. But the most striking feature is very good water stability and easy to prepare in large quantities in practical application. It has a broad application prospect for pollutant removal in water environment.

3.4. Adsorption Thermodynamics. To investigate the adsorption thermodynamics, the adsorption experiments were performed at different temperatures. The parameters of thermodynamics are given in Table 4; the negative value of ΔH^θ suggested exothermic reaction in the process of adsorption, while negative ΔS^θ suggested that there was a decrease in randomness at the solid/solution interface during the adsorption of Cr (VI) onto the Cu (I)-MOF. Importantly, the spontaneous degree of reaction was estimated by the Gibbs energy (ΔG): $\Delta G < 0$, spontaneous; $\Delta G = 0$, equilibrium state; $\Delta G > 0$, not spontaneous. The values of ΔG were less than zero in the temperature range of 288–328 K. Their absolute values decreased with an increase of temperature, which implied that the reaction was spontaneous, and the increasing temperatures were unfavorable to adsorption.

3.5. Adsorption Mechanism. The kinetic results were well fitted to the pseudo-second-order model, which indicated that Cr (VI) adsorbed by Cu (I)-MOF belongs to the chemisorption instead of physical adsorption. Chemisorption includes chemical bonding, coordination bonding, acid-base interactions, and ion exchange [18]. First, the possibility of chemical bonding can be ruled out because the chemical valence states of C, N, and Cu in MOF materials did not change before and after adsorption. Second, coordination bonds are not possible because the central coordination atom Cu is already saturated [20]. Third, for acid-base interaction, it is even less likely because there are no other cations in the system except for H^+, only nitrate in the MOF material, and chromate ions in water. Therefore, the ion exchange was the most likely adsorption mechanism in aqueous solution.

For one thing, Cu (I)-MOF is rich in NO_3^- ion; on the other hand, the pH-dependent of increased Cr (VI) adsorption indicated that $HCrO^{4-}$ ion was adsorbed into Cu (I)-MOF. Because, the Cr (VI) ions exist in the form of $HCrO_4^-$ and CrO_4^{2-} in aqueous solutions as follows:

$$\begin{aligned} Cr_2O_7^{2-} + H_2O &\rightleftharpoons 2HCrO_4^-, \quad Ka = 10^{-2.2} \\ HCrO_4^- &\rightleftharpoons CrO_4^{2-} + H+, \quad Ka = 10^{-6.49} \end{aligned} \tag{11}$$

The chromates mainly exist in the form of $HCrO_4^-$ under acidic conditions ($2.2 < pH < 6.49$), while it exists in the form of CrO_4^{2-} at $pH > 6.49$. To sum up, Cr (VI) ions exist in the form of $HCrO_4^-$ at pH of 6.0 in water.

Both the results of infrared spectra and X-ray photoelectron spectroscopy (XPS) supported the ion exchange pathway. In detail, the peak of NO_3^- weakened at 1368 cm^{-1} [20] in the IR spectra, while a new peak of $HCrO_4^-$ appeared at 918 cm^{-1} [19] (Figure 5) suggested that the ion exchanges were partly happened during the adsorption process. Furthermore, the new peak corresponding to Cr 2p in XPS was clearly appeared after Cr (VI) adsorption onto Cu (I)-MOF material (Figure 6(a)). In addition, the high-resolution XPS spectrum illustrated that the peak at 576.78 and 587.28 eV, corresponding to the Cr $2p_{3/2}$ orbital peak, was considered to be Cr (III) [37], and the peak at 578.58 and 587.68 eV, corresponding to the Cr $2p_{1/2}$ orbital peak, was considered to be Cr (VI) (Figure 6(b)). These results implied that a portion of Cr (VI) was reduced to Cr (III) after being adsorbed by Cu (I)-MOF under acidic condition. Above results clearly showed that ion exchange successfully occurred during the process of adsorption.

3.6. Stability. The stability of Cu (I)-MOF was assessed through three cycles of adsorption. As shown in Figure 7, the X-ray diffraction (XRD) spectra of Cu (I)-MOF before and after Cr (VI) adsorption showed similar patterns after three cycles. It was only that some peaks were less intense, indicating that the basic framework of the Cu (I)-MOF did not change after Cr (VI) adsorption. Furthermore, as shown in SEM images (Figure 8), the framework of Cu (I)-MOF was not obvious collapse and decomposition. These results suggested that Cu (I)-MOF as a new type of adsorbent can play an important role in removing Cr (VI) in water at least three cycles.

Table 3: Comparison of adsorption performance parameters of Cr (VI)with other MOF materials in aqueous solution.

MOFs materials	Optimal pH	Equilibrium time/min	Adsorption capacity/mg·g^{-1}	References
ZIF-67	5	20–60	15	[31]
Fe_3O_4@MIL–100 (Fe)	2	120	18	[32]
EDTA-chitosan/Cu-BTC	2	120	47	[33]
Cu-BTC	7	—[a]	50	[17]
Chitosan-MOF	2	480	94	[34]
Cu (I)-MOF	6	180	96	This study
TMU-30	5.6	10	145	[35]
Cu (II)-MOF	6	—	190	[19]
ZJU–101	—	31.6	245	[36]

—[a] means not reported.

Table 4: Thermodynamic parameters for Cr (VI) adsorption onto Cu (I)-MOF in aqueous solution.

Metal	ΔH^θ/kJ·mol^{-1}	ΔS^θ/J·mol^{-1}·K^{-1}	R^2	ΔG^θ/kJ·mol^{-1}				
				T (K)	288	298	308	318	328
Cr (VI)	−8.030	−6.505	0.9998		−6.156	−6.091	−6.026	−5.961	−5.896

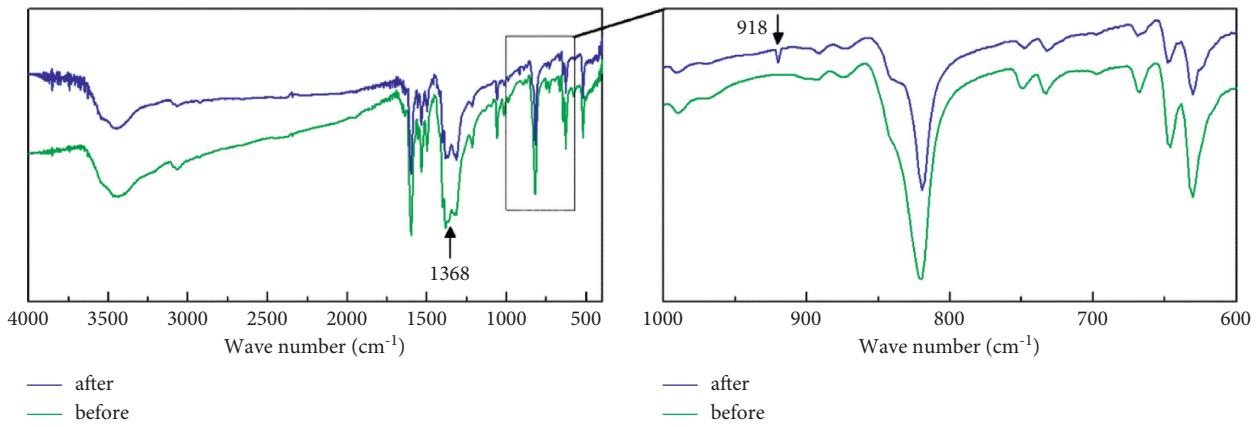

Figure 5: Infrared spectra of Cu (I)-MOF before and after Cr (VI) adsorption.

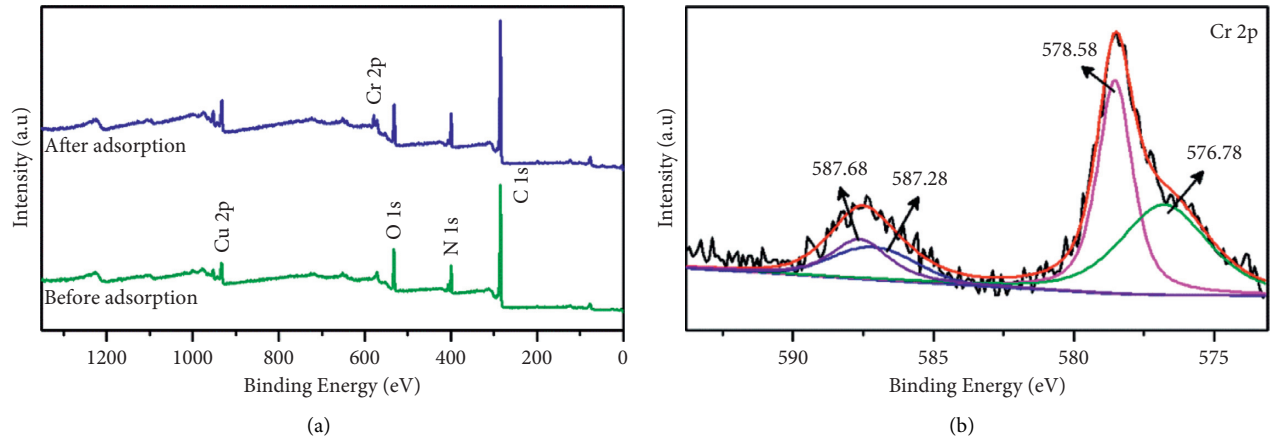

Figure 6: (a) Full-scan XPS spectra of Cu (I)-MOF before and after Cr (VI) adsorption. (b) High-resolution XPS spectra of Cr 2p after adsorption.

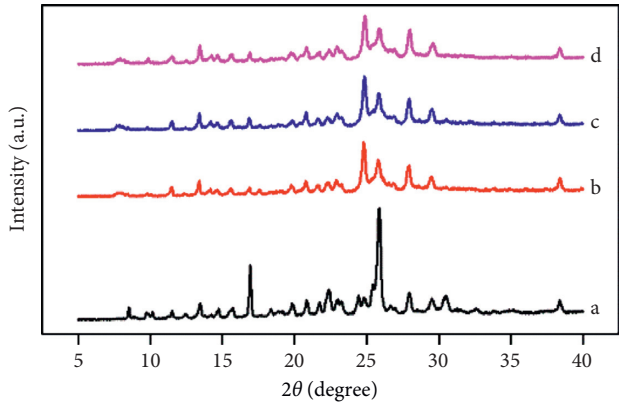

Figure 7: PXRD spectra of Cu (I)-MOF before (a) and after Cr (VI) adsorption through one cycle (b), two cycles (c), and three cycles (d).

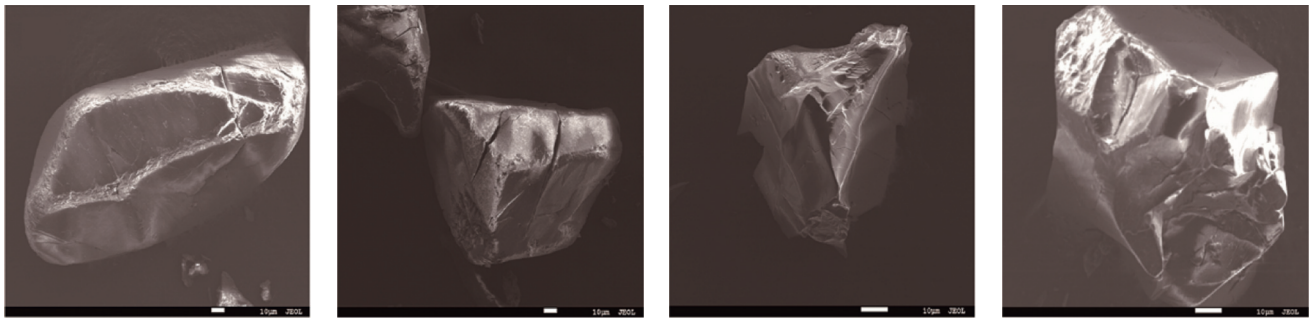

(a) (b) (c) (d)

Figure 8: SEM images of Cu (I)-MOF before (a) and after Cr (VI) adsorption through (b) one cycle, (c) two cycles, and (d) three cycles.

4. Conclusion

The Cr (VI) absorbed by the Cu (I)-MOF was investigated for the optimization, isotherm, kinetics, thermodynamics, and mechanism. First, the optimal pH was 6, the optimal amount of adsorbent was 0.45 $g{\cdot}L^{-1}$, and the adsorption saturation time was 180 min, respectively. Second, the kinetics results revealed that the adsorption of chromium (VI) followed the pseudo-first-order model. Third, the isotherm study indicated that the Langmuir isotherm was the excellent match model. It belongs to a monolayer adsorption, and the maximum adsorption capacity was 95.92 $mg{\cdot}g^{-1}$. Fourth, the thermodynamic parameters of the adsorption demonstrated that the reaction was spontaneous at the temperature range of 288–328 K. Finally, both infrared and XPS results supported the adsorption mechanism was the ion exchange pathway in water. In conclusion, Cu (I)-MOF material has a large of adsorption capacity, good water stability, low cost, and easy to prepare in large quantities in practical application. It will expect the removal of Cr (VI) ions from water as a new type of adsorbent. In the actual treatment, it can be used for the advanced treatment of the wastewater or the purification system of domestic supply water.

Data Availability

The data used to support the findings of this study are included within this article.

Conflicts of Interest

The authors declare that there are no conflicts of interest.

Acknowledgments

This work was supported by the Scientific and Technological Innovation Programs of Higher Education Institutions in Shanxi, China (2020L0584), the Natural Science Foundation of Shanxi Province, China (201901D111299), the Program for "1331 Project" Key Innovative Research Team of Shanxi Province, China (PY201817), the Program for "1331 Project" Key Innovative Research Team of Jinzhong University (jzxycxtd2017007), and the Program for "1331 Project" Maker Team of Jinzhong University (jzxycktd2019031).

References

[1] V. Kumar, R. D. Parihar, A. Sharma et al., "Global evaluation of heavy metal content in surface water bodies: a meta-analysis using heavy metal pollution indices and multivariate statistical analyses," *Chemosphere*, vol. 236, p. 124364, 2019.

[2] IARC (International Agency for Research on Cancer), *Agents Classified by the IARC Monographs*, IARC, Lyon, France, 2021, https://monographs.iarc.who.int/agents-classified-by-the-iarc/.

[3] K. Salnikow and A. Zhitkovich, "Genetic and epigenetic mechanisms in metal carcinogenesis and cocarcinogenesis:

nickel, arsenic, and chromium," *Chemical Research in Toxicology*, vol. 21, no. 1, pp. 28–44, 2008.

[4] S. Chowdhury, M. A. J. Mazumder, O. Al-Attas, and T. Husain, "Heavy metals in drinking water: occurrences, implications, and future needs in developing countries," *The Science of the Total Environment*, vol. 569-570, pp. 476–488, 2016.

[5] L. Keith and W. Telliard, "ES&T Special Report: priority pollutants: I-a perspective view," *Environmental Science and Technology*, vol. 13, no. 4, pp. 416–423, 1979.

[6] Y.-J. Hong, W. Liao, Z.-F. Yan et al., "Progress in the research of the toxicity effect mechanisms of heavy metals on freshwater organisms and their water quality criteria in China," *Journal of Chemistry*, vol. 2020, Article ID 9010348, 12 pages, 2020.

[7] M. Owlad, M. K. Aroua, and A. Wan, "Removal of hexavalent chromium-contaminated water and wastewater: a review," *Water, Air, and Soil Pollution*, vol. 200, no. 1–4, pp. 59–77, 2009.

[8] J. Yang, B. Huang, and M. Lin, "Adsorption of hexavalent chromium from aqueous solution by a chitosan/bentonite composite: isotherm, kinetics, and thermodynamics studies," *Journal of Chemical & Engineering Data*, vol. 65, no. 5, pp. 2751–2763, 2020.

[9] C. Lei, C. Wang, W. Chen, M. He, and B. Huang, "Polyaniline@magnetic chitosan nanomaterials for highly efficient simultaneous adsorption and in-situ chemical reduction of hexavalent chromium: removal efficacy and mechanisms," *The Science of the Total Environment*, vol. 733, p. 139316, 2020.

[10] J. Lee, J.-A. Park, H.-G. Kim et al., "Most suitable amino silane molecules for surface functionalization of graphene oxide toward hexavalent chromium adsorption," *Chemosphere*, vol. 251, p. 126387, 2020.

[11] J. Wu, M. Yan, S. Lv et al., "Preparation of highly dispersive and antioxidative nano zero-valent iron for the removal of hexavalent chromium," *Chemosphere*, vol. 262, p. 127733, 2021.

[12] T. He, Y.-Z. Zhang, X.-J. Kong et al., "Zr(IV)-Based metal-organic framework with T-shaped ligand: unique structure, high stability, selective detection, and rapid adsorption of Cr2O72- in water," *ACS Applied Materials & Interfaces*, vol. 10, no. 19, pp. 16650–16659, 2018.

[13] Z. Zhang, S. Zhang, Q. Yao, G. Feng, M. Zhu, and Z.-H. Lu, "Metal-organic framework immobilized RhNi alloy nanoparticles for complete H2 evolution from hydrazine borane and hydrous hydrazine," *Inorganic Chemistry Frontiers*, vol. 5, no. 2, pp. 370–377, 2018.

[14] K. Yang, K. Yang, S. Zhang, Y. Luo, Q. Yao, and Z.-H. Lu, "Complete dehydrogenation of hydrazine borane and hydrazine catalyzed by MIL-101 supported NiFePd nanoparticles," *Journal of Alloys and Compounds*, vol. 732, pp. 363–371, 2018.

[15] J. Shi, F. Qiu, W. Yuan, M. Guo, and Z.-H. Lu, "Nitrogen-doped carbon-decorated yolk-shell CoP@FeCoP micropolyhedra derived from MOF for efficient overall water splitting," *Chemical Engineering Journal*, vol. 403, p. 126312, 2021.

[16] H. Shayegan, G. A. M. Ali, and V. Safarifard, "Recent progress in the removal of heavy metal ions from water using metal-organic frameworks," *Chemistry*, vol. 5, no. 1, pp. 124–146, 2020.

[17] A. Maleki, B. Hayati, M. Naghizadeh, and S. W. Joo, "Adsorption of hexavalent chromium by metal organic frameworks from aqueous solution," *Journal of Industrial and Engineering Chemistry*, vol. 28, pp. 211–216, 2015.

[18] L. Rani, J. Kaushal, A. L. Srivastav, and P. Mahajan, "A critical review on recent developments in MOF adsorbents for the elimination of toxic heavy metals from aqueous solutions," *Environmental Science and Pollution Research*, vol. 27, no. 36, pp. 44771–44796, 2020.

[19] Z. Shao, C. Huang, Q. Wu et al., "Ion exchange collaborating coordination substitution: more efficient Cr(VI) removal performance of a water-stable CuII-MOF material," *Journal of Hazardous Materials*, vol. 378, p. 120719, 2019.

[20] Y.-Q. Chen, G.-R. Li, Z. Chang, Y.-K. Qu, Y.-H. Zhang, and X.-H. Bu, "IA Cu(i) metal-organic framework with 4-fold helical channels for sensing anions," *Chemical Science*, vol. 4, no. 9, pp. 3678–3682, 2013.

[21] S. Sen Gupta and K. G. Bhattacharyya, "Kinetics of adsorption of metal ions on inorganic materials: a review," *Advances in Colloid and Interface Science*, vol. 162, no. 1-2, pp. 39–58, 2011.

[22] Y. S. Ho and G. McKay, "Pseudo-second order model for sorption processes," *Process Biochemistry*, vol. 34, no. 5, pp. 451–465, 1999.

[23] F. C. Wu, R. L. Tseng, and R. S. Juang, "Characteristics of Elovich equation used for the analysis of adsorption kinetics in dye-chitosan systems," *Chemical Engineering Journal*, vol. 150, no. 2-3, pp. 366–373, 2009.

[24] F. Wu, R. L. Tseng, and R. S. Juang, "Initial behavior of intraparticle diffusion model used in the description of adsorption kinetics," *Chemical Engineering Journal*, vol. 153, no. 1–3, pp. 1–8, 2009.

[25] I. Langmuir, "The adsorption of gases on plane surfaces of glass, mica and platinum," *Journal of the American Chemical Society*, vol. 40, no. 9, pp. 1361–1403, 1918.

[26] H. Freundlich, "Over adsorption in solution," *Journal of Physical Chemistry*, vol. 57, no. 4, pp. 385–471, 1906.

[27] E. C. Lima, F. Sher, M. R. Saeb, M. Abatal, and M. K. Seliem, "Comments on "Reasonable calculation of the thermodynamic parameters from adsorption equilibrium constant, Journal of Molecular Liquids 322 (2021) 114980."," *Journal of Molecular Liquids*, vol. 334, p. 116542, 2021.

[28] D. Zhao, X. Gao, C. Wu, R. Xie, S. Feng, and C. Chen, "Facile preparation of amino functionalized graphene oxide decorated with Fe3O4 nanoparticles for the adsorption of Cr(VI)," *Applied Surface Science*, vol. 384, pp. 1–9, 2016.

[29] M. Janmohammadi, M. Baghdadi, T. M. Adyel, and N. Mehrdadi, "Waste plastic filter modified with polyaniline and polypyrrole nanoparticles for hexavalent chromium removal," *The Science of the Total Environment*, vol. 752, p. 141850, 2021.

[30] E. C. Lima, F. Sher, A. Guleria et al., "Is one performing the treatment data of adsorption kinetics correctly?" *Journal of Environmental Chemical Engineering*, vol. 9, no. 2, p. 104813, 2021.

[31] X. Li, X. Gao, L. Ai, and J. Jiang, "Mechanistic insight into the interaction and adsorption of Cr(VI) with zeolitic imidazolate framework-67 microcrystals from aqueous solution," *Chemical Engineering Journal*, vol. 274, pp. 238–246, 2015.

[32] Q. Yang, Q. Zhao, S. Ren, Q. Lu, X. Guo, and Z. Chen, "Fabrication of core-shell Fe3O4@MIL-100(Fe) magnetic microspheres for the removal of Cr(VI) in aqueous solution," *Journal of Solid State Chemistry*, vol. 244, pp. 25–30, 2016.

[33] Y.-Y. Deng, X.-F. Xiao, D. Wang, B. Han, Y. Gao, and J.-L. Xue, "Adsorption of Cr(VI) from aqueous solution by ethylenediaminetetraacetic acid-chitosan-modified metal-organic framework," *Journal of Nanoscience and Nanotechnology*, vol. 20, no. 3, pp. 1660–1669, 2020.

[34] K. Wang, X. Tao, J. Xu, and N. Yin, "Novel chitosan-MOF composite adsorbent for the removal of heavy metal ions," *Chemistry Letters*, vol. 45, no. 12, pp. 1365–1368, 2016.

[35] L. Aboutorabi, A. Morsali, E. Tahmasebi, and O. Büyükgüngor, "Metal-organic framework based on iso-nicotinate N-oxide for fast and highly efficient aqueous phase Cr(VI) adsorption," *Inorganic Chemistry*, vol. 55, no. 11, pp. 5507–5513, 2016.

[36] Q. Zhang, J. Yu, J. Cai et al., "A porous Zr-cluster-based cationic metal-organic framework for highly efficient Cr2O72− removal from water," *Chemical Communications*, vol. 51, no. 79, pp. 14732–14734, 2015.

[37] X. Guo, A. Liu, J. Lu et al., "Adsorption mechanism of hexavalent chromium on biochar: kinetic, thermodynamic, and characterization studies," *ACS Omega*, vol. 5, no. 42, pp. 27323–27331, 2020.